

# Template Effects of Metal Cations for Controlling the Regioisomer Distribution on the Photodimerization of *N,N'*-Linked Bis(anthracenecarboxamides)

Hisafumi Hiraga,<sup>[a]</sup> Tatsuya Morozumi,<sup>[a]</sup> and Hiroshi Nakamura<sup>\*[a]</sup>

**Keywords:** Anthracene derivatives / Conformation analysis / Host–guest systems / Photochemistry / Photodimerization

Two bis(fluorophore) compounds linked by an oxyethylene chain, *N,N'*-(4,7,10-trioxatridecane-1,13-diyl)bis(1-anthracenecarboxamide) (**1**) and *N,N'*-(4,7,10-trioxatridecane-1,13-diyl)bis(2-anthracenecarboxamide) (**2**), were synthesized, and the intramolecular photodimerization of the anthracene units was carried out in acetonitrile solution. The photoproduct ratios of the regioisomers derived from **1** and **2** were quantified in the absence and presence of metal cations. Upon photo-irradiation of **1**, three intramolecular photodimers, *trans* head-to-head dimer **D1**, *cis* head-to-head **D2** and *cis* head-to-tail **D3**, were formed. In the photodimerization of **1**, the presence of Ba<sup>2+</sup> enhanced the formation of **D1**,

whereas Mg<sup>2+</sup> suppressed it. These isomer distributions strongly depended on the structure of the complex induced by the metal cations in the ground state. On the other hand, upon photo-irradiation of **2**, only two photodimers, *cis* head-to-tail dimer **D5** and *cis* head-to-head **D6**, were formed in both the absence and presence of metal cations, and their ratio changed only slightly suggesting that no conformational changes were induced by the complexation with metal cations.

(© Wiley-VCH Verlag GmbH & Co. KGaA, 69451 Weinheim, Germany, 2004)

## Introduction

Over the past few decades, the photodimerization of anthracene and its derivatives has been extensively investigated for use as photochromic materials and/or photo-switchable molecules,<sup>[1–13]</sup> and as a monomer for photopolymerization.<sup>[14–17]</sup> To achieve an effective photodimerization system, a variety of approaches were employed.<sup>[18–28]</sup> For example, Desvergne and co-workers reported the photocyclomerization (intramolecular dimerization) of macrocyclic crown ethers incorporating two 9,10-anthracenediyl subunits in the absence and presence of Na<sup>+</sup> ions in an organic solvent.<sup>[29]</sup> It was observed that the formation of a 2:1 sodium cation/ligand complex induces an increase in the quantum yield of photocycloaddition. Tamaki et al. reported the photodimerization of 2-anthracenesulfonate and -carboxylate in the presence of  $\gamma$ -cyclodextrin in aqueous solution.<sup>[30]</sup> They successfully achieved a large acceleration effect for the reaction through the formation of an inclusion complex which consisted of a 1:2  $\gamma$ -cyclodextrin/anthracenesulfonate stoichiometry. Tung and co-workers reported the photocycloaddition of 9-substituted anthracene derivatives incorporated within Nafion membranes; the Nafion membranes provide a useful medium in which the regioselectivity of the photocycloaddi-

tion of 9-substituted anthracene derivatives can be controlled.<sup>[31,32]</sup>

The photodimerization of 1- or 2-substituted anthracene gives four regioisomers including two chiral isomers that are *cis* head-to-tail and *trans* head-to-head isomers, whereas the reaction of 9-substituted anthracene gives only two regioisomers that are not chiral isomers. The regioselectivity of the products has been rationalized in terms of steric and electrostatic effects between the substituents.<sup>[33]</sup> The photodimerization of anthracene derivatives in the solid state is one of the most extensively used methods to achieve regioselectivity,<sup>[34–36]</sup> although various studies in solution have also been carried out. Ueno et al. reported that photo-irradiation of a bis(anthracenecarboxylate)-appended  $\gamma$ -cyclodextrin yielded an intramolecular cyclodimer.<sup>[37]</sup> A study of the photodimerization of bis(1- and -2-anthracenecarboxylates) linked by various alkyl chains was carried out by De Schryver et al.<sup>[38]</sup> They estimated a regioisomer ratio for the intramolecular cyclodimers derived from the 2-anthracene substrate, but not, unfortunately, from the 1-anthracene substrate. Recently, Nakamura and Inoue studied the photodimerization of 2-anthracenecarboxylic acid in the presence of  $\gamma$ -cyclodextrins.<sup>[39]</sup> They estimated the ability of the cyclodextrin cavity to introduce chirality during the photoreaction of anthracenecarboxylic acid. The mechanism and the factors determining the product ratio and enantiomeric excesses were also discussed.

We have developed a series of chemosensors that consist of mono- or bis(fluorophores) linked by oxyethylene chains of various lengths.<sup>[40–43]</sup> It was found that these chemosen-

<sup>[a]</sup> Division of Materials Science, Graduate School of Environmental Earth Science, Hokkaido University, Sapporo 060-0810, Japan  
Fax: (internat.) + 81-11-706-4863  
E-mail: nakamura@ees.hokudai.ac.jp

sors experienced a conformational change from a linear to a helical structure upon complexation with target molecules, and that the terminal fluorophores moved close to each other. The changes that accompanied the complexation could be observed in fluorescence spectra. It occurred to us that an effective photoreaction system could be developed using a substrate that consists of bis(1- and -2-anthracene) derivatives linked by an oxyethylene chain, and that the distribution of regioisomers produced in the reaction system could be controlled by its complexation with metal cations. Moreover, there is the possibility that chiral transcription into 1- and 2-anthracene photodimers will occur by complexation with a chiral template such as an amino acid. On the basis of this idea, we preliminarily reported on the photoreaction of **1**.<sup>[44]</sup> In this paper, we report the results of the intramolecular photodimerization of **1** and **2**, and the quantitative effect of metal cations on the photoreaction. Changes to the conformation of the **1**-metal cation complex in the ground state that influence the photoproduct ratio are also discussed.

## Results and Discussion

### Template Effects of Metal Cations

After photo-irradiation of **1**, the formation of three products (**D1–D3**) was confirmed by HPLC analysis. These three compounds (regioisomers) were separated by using HPLC, and their structures were determined by 2D NMR, H-H COSY and NOESY spectra. The structures of these compounds are shown in Figure 1. Regioisomer distri-

butions were also determined by the ratio of the peak intensities of the protons at the bridgehead carbon atoms in their <sup>1</sup>H NMR spectra, and are summarized in Table 1. The ratio of regioisomers was evaluated in the same way for products from the photoreaction of **2**. The photodimerization of **1** in the absence of metal cations gave the regioisomers in a ratio of **D1/D2/D3** = 32:57:11. The formation of *trans* head-to-tail isomer **D4** was not detected, indicating that the chain of **1** is not long enough to allow the formation of **D4**. These isomer ratios suggest that **1** prefers the anthracene moieties to be stacked in the *cis* head-to-head or *trans* head-to-head conformer. These conformers can also be considered to have little steric strain around the oxyethylene moiety.

Table 1. Isomer ratio (%) of the photodimers of **1–3** before and after complexation with various cations

Ligand	Cation <sup>[a]</sup>	<i>trans</i> h-h <sup>[b]</sup>	<i>cis</i> h-h <sup>[b]</sup>	<i>cis</i> h-t <sup>[c]</sup>	<i>trans</i> h-t <sup>[c]</sup>
<b>1</b>		<b>D1</b>	<b>D2</b>	<b>D3</b>	<b>D4</b>
	none	31.9	57.0	11.1	— <sup>[d]</sup>
	Mg <sup>2+</sup>	16.5	81.3	2.2	— <sup>[d]</sup>
	Ca <sup>2+</sup>	24.7	74.1	1.2	— <sup>[d]</sup>
	Sr <sup>2+</sup>	40.9	59.0	0.1	— <sup>[d]</sup>
	Ba <sup>2+</sup>	45.7	54.2	0.1	— <sup>[d]</sup>
	Li <sup>+</sup>	34.7	56.9	8.4	— <sup>[d]</sup>
	Na <sup>+</sup>	32.6	58.1	9.3	— <sup>[d]</sup>
	K <sup>+</sup>	31.9	58.3	9.8	— <sup>[d]</sup>
<b>2</b>			<b>D6</b>	<b>D5</b>	
	none	— <sup>[d]</sup>	66.0	34.0	— <sup>[d]</sup>
	Mg <sup>2+</sup>	— <sup>[d]</sup>	67.0	33.0	— <sup>[d]</sup>
	Ca <sup>2+</sup>	— <sup>[d]</sup>	66.2	33.8	— <sup>[d]</sup>
	Sr <sup>2+</sup>	— <sup>[d]</sup>	65.7	34.3	— <sup>[d]</sup>
	Ba <sup>2+</sup>	— <sup>[d]</sup>	67.6	32.4	— <sup>[d]</sup>
	Li <sup>+</sup>	— <sup>[d]</sup>	66.1	33.9	— <sup>[d]</sup>
	Na <sup>+</sup>	— <sup>[d]</sup>	66.6	33.4	— <sup>[d]</sup>
	K <sup>+</sup>	— <sup>[d]</sup>	66.2	33.8	— <sup>[d]</sup>
<b>3</b>	none	23.3	20.5	30.4	25.8

<sup>[a]</sup> For Mg<sup>2+</sup> or alkali metal ions, M<sub>1</sub>, [M<sub>1</sub>]/[**1**] or [**2**] = 20, and for other metal cations, M<sub>2</sub>, [M<sub>2</sub>]/[**1**] or [**2**] = 10. <sup>[b]</sup> h-h: head-to-head. <sup>[c]</sup> h-t: head-to-tail. <sup>[d]</sup> Not detected.

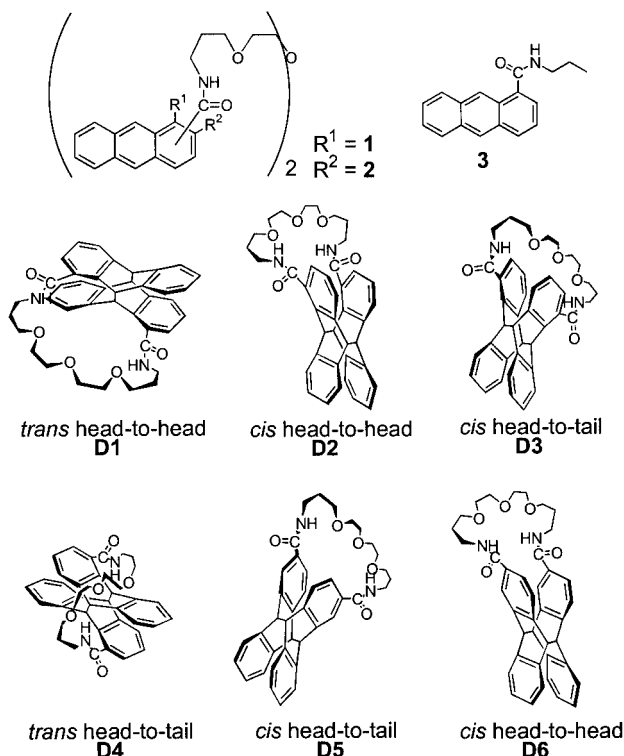


Figure 1. Structures of **1**, **2** and **3** and the photodimers

The effect on the isomer distributions of the complexation of **1** with alkaline earth metal ions was examined in acetonitrile solution. When Mg<sup>2+</sup> was added as a guest for **1**, the formation of **D2** was enhanced, whereas that of **D1** and **D3** was inhibited. As a result, the isomer ratio changed to **D1/D2/D3** = 17:81:2. A similar trend was observed with **1**·Ca<sup>2+</sup>. After the addition of Ba<sup>2+</sup>, however, the formation of **D1** was slightly enhanced, and the isomer ratio changed to **D1/D2/D3** = 46:54:0.1. A similar result was also observed when Sr<sup>2+</sup> was present as a guest for **1**. In general, a larger ionic radius increased the formation of **D1**, and decreased that of **D2**. The formation of **D3** was almost inhibited in all cases. The alkali metal ions did not affect the ratio of the isomers.

To examine the steric effects between the substituents, the intermolecular photodimerization of **3** was carried out in acetonitrile for comparison. Because of the second-order

reaction kinetics and the low concentration, the reaction rate of **3** was slow. The ratios of the four isomers produced in the photodimerization of **3** were evaluated, and are also listed in Table 1. The product ratio of *cis* head-to-head isomer was lower (20.5%) than that of the other three isomers. This shows that upon photodimerization the substituents tend to avoid heavy congestion to reduce the steric effects.

Upon irradiation of **2** in the absence of metal cations, the ratio of the regioisomers was evaluated as **D5/D6** = 34:66 in an acetonitrile solution containing 10% DMF. The *trans* head-to-head and *trans* head-to-tail isomers were not detected due to the fact that the chain of **2** is not long enough to allow the formation of these isomers. The present result is quite similar to those of De Schryver et al.<sup>[38]</sup>

The addition of alkaline earth metal ions to a solution of **2** can also be expected to change the isomer ratio. The addition of metal cations to a solution of **2** induced a change in the chemical shifts in the <sup>1</sup>H NMR spectra which shows clear evidence of complexation with these metal cations, as mentioned below. However, the formation of the **2**:alkaline earth metal ion complex did not affect the isomer distributions. These results indicate that the conformation of the organic component of this complex is similar to that of free **2** before photodimerization. No change in the ratio of regioisomers was observed on addition of alkali metal ions to **2**, similar to the case of **1**.

### Spectral Properties

Ligand **1** exhibits a monomer emission with  $\lambda_{\text{max.}} = 435$  nm, as shown in Figure 2. This assignment of the emission species is supported by the fluorescence spectrum of reference compound **3** which has a similar monomer emission but a significantly higher fluorescence intensity, as depicted in Figure 3. The fluorescence spectra of **1** in the presence of a large excess of various metal cations were also measured. With the alkaline earth metal ions, a significant increase in the fluorescence intensity was observed when  $\text{Mg}^{2+}$  was added as a guest for **1**. On the other hand, a decrease in the monomer emission intensities and an in-

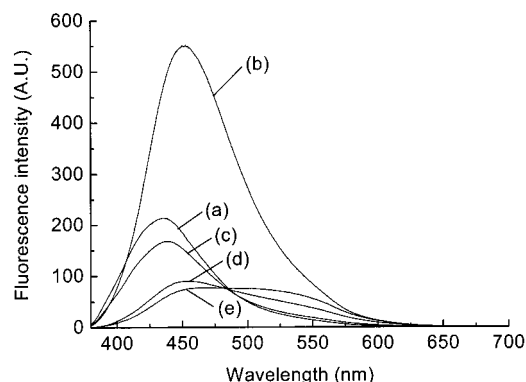


Figure 2. Corrected fluorescence spectra of **1** (a), **1** +  $\text{Mg}(\text{ClO}_4)_2$  (b), **1** +  $\text{Ba}(\text{ClO}_4)_2$  (c), **1** +  $\text{Sr}(\text{ClO}_4)_2$  (d) and **1** +  $\text{Ca}(\text{ClO}_4)_2$  (e) in acetonitrile at 25 °C; excitation wavelength: 362 nm;  $[\mathbf{1}] = 1 \times 10^{-5} \text{ mol}\cdot\text{dm}^{-3}$ ,  $[\text{Mg}(\text{ClO}_4)_2] = 2 \times 10^{-4} \text{ mol}\cdot\text{dm}^{-3}$ ,  $[\text{Ba}(\text{ClO}_4)_2] = [\text{Sr}(\text{ClO}_4)_2] = [\text{Ca}(\text{ClO}_4)_2] = 1 \times 10^{-4} \text{ mol}\cdot\text{dm}^{-3}$ .

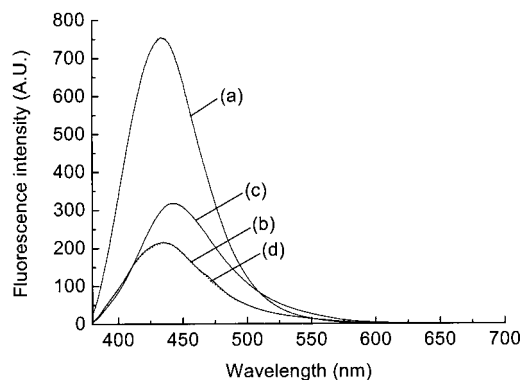


Figure 3. Corrected fluorescence spectra of reference compound **3** (a), **1** (b), **1** +  $\text{LiClO}_4$  (c) and **1** +  $\text{NaClO}_4$  (d) in acetonitrile at 25 °C; excitation wavelength: 362 nm;  $[\mathbf{1}] = 1 \times 10^{-5} \text{ mol}\cdot\text{dm}^{-3}$ ,  $[\text{LiClO}_4] = [\text{NaClO}_4] = 1 \times 10^{-3} \text{ mol}\cdot\text{dm}^{-3}$ .

crease in the excimer (anthracene–anthracene\*) emission intensities, which are located in the region of 500–600 nm, were observed when  $\text{Ca}^{2+}$ ,  $\text{Sr}^{2+}$  and  $\text{Ba}^{2+}$  were added as a guest for **1**. With the exception of  $\mathbf{1}\cdot\text{Mg}^{2+}$ , the excimer emission intensity gradually increased as the ionic radius of the guest decreased. These considerations are discussed in detail in the “Conformational Changes of Ligands Effected by Metal Cations” section.

With the alkali metal ions, an increase in the fluorescence intensity was observed on addition of a large excess of  $\text{Li}^+$ , as shown in Figure 3. However, almost no spectral change was observed even when a 100-fold equivalent of  $\text{Na}^+$  was added to **1**. These observations indicate that  $\text{Li}^+$  interacts to a limited extent with **1**, but  $\text{Na}^+$  interacts very little.

On the other hand, the fluorescence spectra of **2** in the absence and presence of a large excess of various metal cations were also measured. However, no significant change in the fluorescence intensity was observed when any metal cations were added as a guest for **2**, indicating that there was no change in the isomer ratio.

### Quantum Yields for Photodimerization

The quantum yields  $\Phi$  for the photodimerization of **1** were determined to quantify the effect of metal cations on the reaction, as depicted in Table 2. The values of  $\Phi$  were

Table 2. Quantum yields for the photodimerization of **1** and **2**

Cation	<b>1</b>				<b>2</b>		
	$\Phi_{\text{total}}$	$\Phi_{\text{D1}}$ [a]	$\Phi_{\text{D2}}$ [a]	$\Phi_{\text{D3}}$ [a]	$\Phi_{\text{total}}$	$\Phi_{\text{D5}}$ [a]	$\Phi_{\text{D6}}$ [a]
none	0.301	0.096	0.172	0.033	0.255	0.087	0.168
$\text{Mg}^{2+}$	0.226	0.037	0.184	0.005	0.228	0.075	0.153
$\text{Ca}^{2+}$	0.305	0.075	0.226	0.004	0.246	0.083	0.163
$\text{Ba}^{2+}$	0.327	0.149	0.177	0.001	0.313	0.101	0.212

[a]  $\Phi_{\text{D1–D6}} = \Phi_{\text{total}} \times \text{isomer ratio (D1–D6)}$ .

evaluated from the decay of the absorbance of **1**, shown in Figure 4, according to literature methods.<sup>[40]</sup>

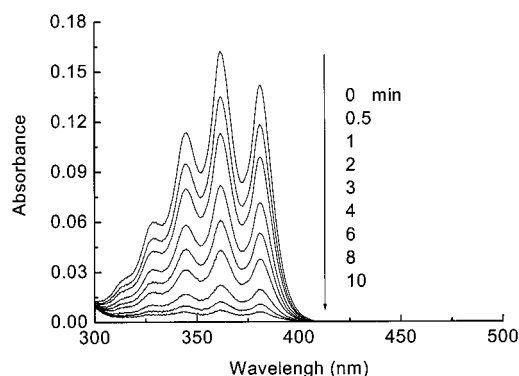


Figure 4. Changes in the absorption spectra of **1** with time on irradiation with a 500-W Xe lamp (350 nm, 0.4 mW·cm<sup>-2</sup>)

The total quantum yields  $\Phi_{\text{total}}$  for the photodimerization of **1** were almost the same ( $\Phi_{\text{total}} \approx 0.3$ ) in all experiments. The photodimerization of **1** was not accelerated or retarded by the addition of metal cations. However, the value of  $\Phi_{\text{D1}}$  for **1**·Ba<sup>2+</sup> was 1.5 times greater than that for free **1**, whereas the value of  $\Phi_{\text{D2}}$  was almost the same as that for free **1** and  $\Phi_{\text{D3}}$  was almost zero. This means that Ba<sup>2+</sup> enhanced the generation of **D1**, had no effect on **D2**, and completely depressed the formation of **D3**. Thus, the value of  $\Phi_{\text{total}}$  was slightly increased. After the addition of Mg<sup>2+</sup>, the value of  $\Phi_{\text{D1}}$  was 0.38 times smaller than that of free **1**, whereas  $\Phi_{\text{D2}}$  was unchanged and  $\Phi_{\text{D3}}$  much smaller. Hence, the  $\Phi_{\text{total}}$  was decreased. Note that the high selectivity for **D2** in **1**·Mg<sup>2+</sup> originates from the suppression of the formation of **D1** and **D3** by Mg<sup>2+</sup>.

The quantum yields  $\Phi$  for the photodimerization of **2** are also shown in Table 2. The total quantum yield  $\Phi_{\text{total}}$  for the photodimerization of **2** was 0.255 before complexation with metal cations. This value is lower than that for **1**, which indicates that it is slightly more difficult for **2** to adopt the *cis* head-to-head conformation than it is for **1**. Furthermore, the value of  $\Phi_{\text{total}}$  increased in the presence of Ba<sup>2+</sup>, but decreased on complexation with Mg<sup>2+</sup>.

### Complex Formation Constants

The photodimerization of **1** was facilitated even by irradiation with the excitation light during the fluorescence measurements. Therefore, a <sup>1</sup>H NMR titration was carried out. The complex formation constants (*K*) for **1**·metal cation complexes in [D<sub>3</sub>]acetonitrile, which is defined by Equation (1), were determined from the curve of the chemical shift changes by means of a nonlinear least-squares curve-fitting method (Marquardt's method).<sup>[45]</sup> Complex formation constants for **2**·metal cation complexes could not be determined because of the very low solubility of **2** in [D<sub>3</sub>]acetonitrile.

$$K = [\text{M} \cdot \text{L}] / [\text{M}][\text{L}] \quad (1)$$

The complex formation constants (log *K*) for the **1**·alkaline earth metal ion complexes were calculated to demonstrate the binding ability of the cations, and are listed in Table 3. In the case of **1**·Ca<sup>2+</sup>, the value exceeded the experimental limitations of the <sup>1</sup>H NMR measurements and titration curve-fitting and so could not be determined. However, this result does suggest that the actual complex formation constant value for **1**·Ca<sup>2+</sup> is larger than the value given in Table 3. The complex formation constants for the **1**·alkali metal ion complexes were also calculated. These values for **1**·Li<sup>+</sup> and, in particular, for **1**·Na<sup>+</sup> are lower than the values for the **1**·alkaline earth metal ions. Thus, these results indicate that Li<sup>+</sup> interacts slightly with **1**, and that Na<sup>+</sup> only interacts poorly with **1**, and are in accord with the spectral observations noted above.

Table 3. Complex formation constants of **1** with various cations

	Mg <sup>2+</sup>	Ca <sup>2+</sup>	Sr <sup>2+</sup>	Ba <sup>2+</sup>	Li <sup>+</sup>	Na <sup>+</sup>
log <i>K</i>	3.97	> 6.00	5.56	5.41	2.26	1.39

### Conformational Changes of Ligands Effected by Metal Cations

To consider the effect of metal cations on the photodimerization of **1** in the ground state and the factors determining the regioisomer ratio, **1** was studied by <sup>1</sup>H NMR spectroscopy in the absence and presence of metal cations in [D<sub>3</sub>]acetonitrile. The <sup>1</sup>H NMR spectra of **1** before and after the addition of Ca<sup>2+</sup> ions are depicted in Figure 5 as a typical result. Peak assignments were made by using the H-H COSY and NOESY spectra. The chemical shifts of **1** and the chemical shift changes induced by the formation of complexes with various metal cations are listed in Table 4.

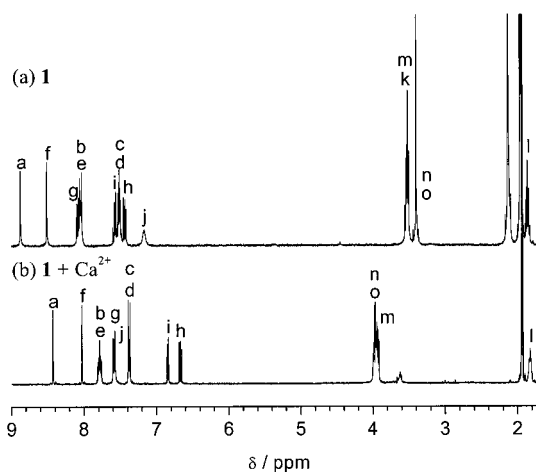
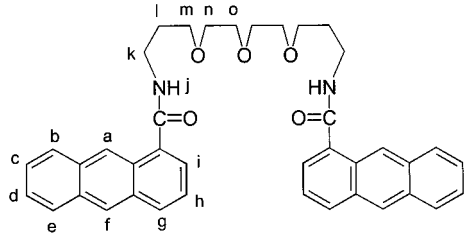


Figure 5. <sup>1</sup>H NMR spectra of **1** in [D<sub>3</sub>]acetonitrile at 30 °C before (a) and after (b) the addition of Ca<sup>2+</sup>; [**1**] = 1 × 10<sup>-2</sup> mol·dm<sup>-3</sup>, [Ca(ClO<sub>4</sub>)<sub>2</sub>] = 1 mol·dm<sup>-3</sup>



Table 4. Chemical shifts ( $\delta$  [ppm]) for **1** and their changes upon complexation with various cations

															
Cation <sup>[a]</sup>	a	b	c	d	e	f	g	h	i	j	k	l	m	n	o
none	8.85	8.02	7.49	7.49	8.02	8.49	8.06	7.41	7.54	7.14	3.49	1.83	3.49	3.38	3.38
Mg <sup>2+</sup>	−0.36	−0.13	0.02	0.02	0.01	−0.03	−0.03	−0.16	−0.23	0.89	0.15	0.14	0.26	0.45	0.45
Ca <sup>2+</sup>	−0.42	−0.22	−0.10	−0.12	−0.24	−0.46	−0.47	−0.74	−0.70	0.44	− <sup>[b]</sup>	0.00	0.45	0.59	0.59
Sr <sup>2+</sup>	−0.25	−0.23	−0.18	−0.11	−0.18	−0.38	−0.38	−0.61	−0.54	0.43	0.19	0.03	0.42	0.53	0.53
Ba <sup>2+</sup>	−0.16	−0.26	−0.22	−0.10	−0.14	−0.27	−0.24	−0.40	−0.31	0.44	0.17	0.07	0.35	0.46	0.46
Li <sup>+</sup>	−0.09	−0.14	−0.05	−0.05	−0.02	−0.05	−0.02	−0.06	−0.04	0.31	0.02	−0.01	0.12	0.30	0.30
Na <sup>+</sup>	−0.16	−0.08	−0.03	−0.03	−0.08	−0.12	−0.12	−0.13	−0.17	0.00	−0.16	0.03	0.10	0.25	0.25

<sup>[a]</sup> Positive values show lower field shifts, and negative values show higher field shifts. The values in “none” indicate the chemical shifts ( $\delta$  [ppm], from TMS) of the protons of **1** in [D<sub>3</sub>]acetonitrile at 30 °C. <sup>[b]</sup> This value could not be assigned owing to overlapping by the peak due to water.

After the addition of metal cations, the oxyethylene protons (m–o and k) and the amide proton j in **1** showed lower magnetic field shifts in all cases, indicating that **1** binds to metal cations through the oxyethylene moiety and the amide carboxy group cooperatively. In the cases of **1**·Ca<sup>2+</sup>, **1**·Sr<sup>2+</sup> and **1**·Ba<sup>2+</sup>, significantly higher magnetic field shifts were observed for all of the anthracene ring protons (a–i) indicating a deshielding effect due to stacking of the anthracene rings. The shift values for each proton decreased as the ionic radii increased [e.g., proton i:  $\Delta\delta$  = −0.70 (Ca<sup>2+</sup>), −0.54 (Sr<sup>2+</sup>), −0.31 (Ba<sup>2+</sup>) ppm]. The decrease in shift values shows that the distance between the anthracene rings increases as the ionic radii of the guest cations increases.

On the basis of these results, the existence of different conformers can be expected. The **1**·Ca<sup>2+</sup> complex has a well-defined face-to-face conformer as shown in Figure 6 (a). The structures of **1**·Sr<sup>2+</sup> and **1**·Ba<sup>2+</sup> should be similar to that of **1**·Ca<sup>2+</sup>. This conformer could allow the generation of the isomer **D2**, and suppress the formation of **D3**. On the other hand, complexation with Ba<sup>2+</sup> further enhanced the generation of **D1**. The formation of the **D1** isomer can be best explained by rotation around the anthracene–C=O bond axis in the excited state and/or during the dimerization as depicted in Figure 6 (b). In the case of **1**·Ca<sup>2+</sup>, the two anthracene rings come close to each other, and steric hindrance should arise, suppressing the rotation of the ring that would lead to the formation of the **D1** isomer. As the ionic radius increases, the steric hindrance will decrease as the distance between the two anthracene rings increases. The rotation becomes easier, and the conformer (*trans* head-to-head) that leads to **D1** may be preferred. As a result, the formation of the **D1** isomer is enhanced in the photoreaction of **1**·Ba<sup>2+</sup>. These interpretations are consistent with fluorescence spectral observations.

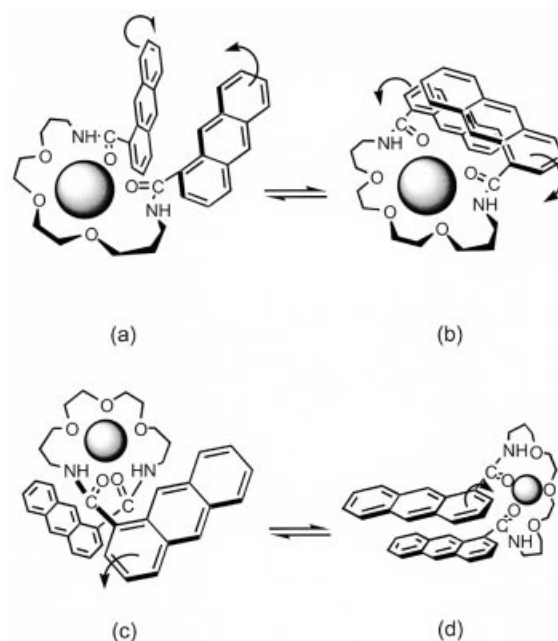


Figure 6. Schematic representation of the expected structures of **1**·Ca<sup>2+</sup> (a), (b) and **1**·Mg<sup>2+</sup> (c), (d) complexes

The **1**·Mg<sup>2+</sup> complex showed small higher magnetic field shift changes at proton a, h and i ( $\Delta\delta$  = −0.36, −0.16 and −0.23 ppm, respectively) and a large lower magnetic field shift change at amide proton j ( $\Delta\delta$  = 0.89 ppm). This indicates that the  $\pi$ – $\pi$  interaction in **1** is quite small whereas the electrostatic interaction between the carbonyl group and Mg<sup>2+</sup> is large upon complexation. The best fitted structure of **1**·Mg<sup>2+</sup> has a “roll-up” conformation as shown in Figure 6 (c). Although the rolled-up conformer can be regarded as having no significant advantage for the reaction, the photodimerization of **1**·Mg<sup>2+</sup> gave the **D2** isomer with

high selectivity. The rotation around the anthracene–C=O bond axis in the excited state is also displayed in Figure 6 (d). The rolled-up conformer of  $1 \cdot \text{Mg}^{2+}$  is highly advantageous for this rotation since the steric hindrance around the two anthracene rings is quite small compared with that in  $1 \cdot \text{Ca}^{2+}$ . Thus, the photodimerization of  $1 \cdot \text{Mg}^{2+}$  gave the **D2** isomer with high selectivity although the rolled-up conformer did not enhance the reaction, there being a slight decrease in the value of  $\Phi_{\text{total}}$  for  $1 \cdot \text{Mg}^{2+}$ . The  $1 \cdot \text{Li}^+$  complex showed lower magnetic field shift changes at the oxyethylene chain protons n and o and at the amide proton j ( $\Delta\delta = 0.30, 0.30$  and  $0.31$  ppm, respectively) as listed in Table 4. On the other hand, smaller chemical shift changes at the anthracene ring protons ( $\Delta\delta \approx 0.1$  ppm) were observed, indicating that  $\text{Li}^+$  did not induce an interaction between the anthracene rings. Therefore, the product ratio of  $1 \cdot \text{Li}^+$  was quite similar to that of free **1**. In the case of  $1 \cdot \text{Na}^+$ , with the exception of proton j, similar results were obtained, and these can also be interpreted in the same way.

In the case of **2**, unfortunately, the  $^1\text{H}$  NMR spectrum of free **2** could not be measured because of its low solubility in  $[\text{D}_3]\text{acetonitrile}$ . In contrast, the  $^1\text{H}$  NMR spectra of the **2**-metal cation complexes could be measured owing to an increase in solubility, and the chemical shifts of these complexes are given in Table 5. Although the structures of the **2**-metal cation complexes are difficult to identify, the chemical shift values in Table 5 clearly show their formation. For example, the chemical shifts of  $2 \cdot \text{Ca}^{2+}$  (protons m and n:  $\delta = 3.85$  and  $3.91$  ppm) were observed, and these values are almost the same as those of  $1 \cdot \text{Ca}^{2+}$  (protons m and n:  $\delta = 3.94$  and  $3.97$  ppm). Similar results were also observed for the complexation of **1** with  $\text{Sr}^{2+}$  or  $\text{Ba}^{2+}$  (Table 5). However, the photoproduct isomer ratios were the same with all the metal ions studied. The most plausible structure is the face-to-face conformation (see a in Figure 7), in which the anthracene ring can rotate around the amide bond axis as shown in Figure 7. Owing to the hydrogen bonding between the amide groups, the formation of **D6** (see a in Figure 7) will be preferred to that of **D5** (see b in Figure 7). The increase in the value of  $\Phi_{\text{total}}$  for  $2 \cdot \text{Ba}^{2+}$  may be due to the template effect of  $\text{Ba}^{2+}$  which can stabilize both conformations.

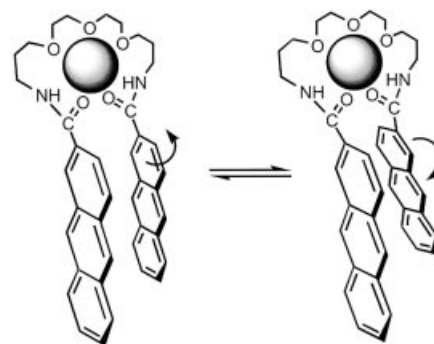


Figure 7. Schematic representation of the expected structures of the **2**-metal complex

## Conclusions

The work described herein has shown that a metal template effect can be used to control the stereochemistry of the photodimerization of 1- and 2-anthracenecarboxamide. Upon photo-irradiation of **1**, three photodimers were formed. The isomer distributions were greatly affected by metal cations, and strongly depended on the structure of the complex induced by the metal cations in the ground state. On the other hand, photo-irradiation of **2** led to the formation of two photodimers. The quantum yields  $\Phi$  for the photodimerization of **1** and **2** indicated high reactivity for the photoreaction. This approach could be suitable for controlling the stereochemistry of photoreactions.

## Experimental Section

**Synthesis of Compounds 1 and 2:** A solution of 1-anthracenecarboxylic acid (1-anthroic acid) (1 mmol) in  $\text{SOCl}_2$  (30 mL) was refluxed for 2 h. Excess  $\text{SOCl}_2$  was distilled off in vacuo, and completely evaporated. The resulting acyl chloride was dissolved in THF (50 mL). Diethylene glycol bis(3-aminopropyl) ether (0.5 mmol) and triethylamine (1 mmol) in THF (50 mL) were gradually added dropwise to this solution in an ice bath and refluxed for 2 h. The solvent was evaporated under reduced pressure, the residue was purified by silica gel column chromatography (eluent  $\text{CHCl}_3$ ) and then recrystallized from ethanol. The crude prod-

Table 5. Chemical shifts ( $\delta$  [ppm]) for the **2**-metal cation complexes

Cation	a	b	c	d	e	f	g	h	i	j	k	l	m	n	o
$\text{Ca}^{2+}$	8.39	7.76	7.55	7.28	7.28	7.62	7.81	7.48	7.62	8.16	3.71	1.88	3.85	3.91	3.91
$\text{Sr}^{2+}$	8.58	7.82	7.41	7.20	7.35	7.75	8.06	7.71	7.81	8.06	3.73	1.87	3.80	3.85	3.85
$\text{Ba}^{2+}$	8.61	8.08	7.53	7.27	7.42	7.86	8.22	7.83	7.83	7.97	3.69	1.89	3.75	3.80	3.80

uct of compound **1** was further purified by HPLC on an ODS column. In a similar way, compound **2** was synthesized from 2-anthracenecarboxylic acid (2-anthroic acid) (1 mmol). In the case of **2**, CH<sub>3</sub>COOH was used as the solvent for recrystallization. The structures and purities of **1** and **2** were confirmed by their <sup>1</sup>H NMR spectra and elemental analyses.

**N,N'-(4,7,10-Trioxatridecane-1,13-diyl)bis(1-anthracenecarboxamide) (1):** Pale yellow solid; m.p. 158–160 °C. <sup>1</sup>H NMR (400 MHz, CDCl<sub>3</sub>, 30 °C): δ = 1.83 (m, 4 H, CCH<sub>2</sub>C), 3.14 (m, 4 H, OCH<sub>2</sub>), 3.17 (m, 4 H, OCH<sub>2</sub>), 3.42 (t, *J* = 6.0 Hz, 4 H, OCH<sub>2</sub>), 3.61 (d, *J* = 6.0 Hz, 4 H, NCH<sub>2</sub>), 6.83 (t, *J* = 5.3 Hz, 2 H, NH), 7.33 (dd, *J* = 8.6, 6.8 Hz, 2 H, aromatic 3-H), 7.45 (m, 4 H, aromatic 6-, 7-H), 7.52 (d, *J* = 6.8 Hz, 2 H, aromatic 2-H), 7.94 (d, *J* = 9.2 Hz, 2 H, aromatic 8-H), 7.97 (d, *J* = 8.4 Hz, 2 H, aromatic 4-H), 7.98 (m, 2 H, aromatic 5-H), 8.37 (s, 2 H, aromatic 10-H), 8.91 (s, 2 H, aromatic 9-H) ppm. <sup>13</sup>C NMR (100 MHz, CDCl<sub>3</sub>, 30 °C): δ = 29.2, 39.0, 70.0, 70.2, 70.49, 123.7, 124.5, 124.7, 125.6, 125.8, 126.5, 127.7, 127.9, 128.7, 130.6, 131.5, 132.0, 134.7, 169.1 ppm. C<sub>40</sub>H<sub>40</sub>N<sub>2</sub>O<sub>5</sub> (628.76): calcd. C 76.41, H 6.41, N 4.46; found C 76.31, H 6.56, N 4.41. MS (ESI): *m/z* = 651.48 [M + Na]<sup>+</sup>.

**N,N'-(4,7,10-Trioxatridecane-1,13-diyl)bis(2-anthracenecarboxamide) (2):** Pale yellow solid; m.p. 246–248 °C. <sup>1</sup>H NMR (400 MHz, CDCl<sub>3</sub>, 30 °C): δ = 1.85 (m, 4 H, CCH<sub>2</sub>C), 3.51–3.64 (m, 16 H, OCH<sub>2</sub>, NCH<sub>2</sub>), 7.26 (t, 2 H, NH), 7.47 (m, 4 H, aromatic 6-, 7-H), 7.78 (dd, *J* = 8.9, 1.7 Hz, 2 H, aromatic 3-H), 7.95–7.98 (m, 6 H, aromatic 4-, 5-, 8-H), 8.37 (s, 2 H, aromatic 9-H), 8.44 (s, 2 H, aromatic 10-H), 8.47 (s, 2 H, aromatic 1-H) ppm. <sup>13</sup>C NMR (100 MHz, CDCl<sub>3</sub>, 30 °C): δ = 29.0, 39.1, 70.2, 70.4, 70.7, 123.1, 125.8, 126.2, 127.9, 128.2, 128.6, 130.6, 131.5, 132.0, 132.7, 167.4 ppm. C<sub>40</sub>H<sub>40</sub>N<sub>2</sub>O<sub>5</sub>·H<sub>2</sub>O (646.78): calcd. C 74.28, H 6.54, N 4.43; found C 74.37, H 6.49, N 4.53. MS (ESI): *m/z* = 651.28 [M + Na]<sup>+</sup>.

**Photoreaction:** The photo-irradiation of a degassed acetonitrile solution of **1** or **2** (1 × 10<sup>−4</sup> M) was carried out by using a USIO 500-W Xenon short arc lamp with a bandpass filter to produce UV light of approximately 350 nm. To determine the quantum yields of the photodimerization reactions, a Jovin Ybon UV-10 monochromator (bandwidth: 16 nm) was used to produce monochromatic light of 350 nm. The light intensity was monitored by using an OPHIR Orion laser power/energy monitor. A thermostated cell holder was used to maintain the temperature at 25 ± 0.1 °C. In all cases, the irradiation was continued until the absorbance at 365 nm decreased to steady values.

**HPLC Analysis:** HPLC analyses were performed using a Shimadzu HPLC 10Avp equipped with tandem columns of Inertsil ODS-2 (250 × 4.6 mm i.d., GL Science) and ULTRON VX-ODS (250 × 4.6 mm i.d., Shinwa Chemical Ind.), and a preparative column of ULTRON VX-ODS (250 × 20 mm i.d., Shinwa Chemical Ind.). A mixture of acetonitrile/water was used as the mobile phase for **1** (80:20, v/v) and **2** (50:50, v/v). The flow rate of the mobile phases was set at 0.5 mL·min<sup>−1</sup> for analysis and 8 mL·min<sup>−1</sup> for preparation. The columns were kept at 25 °C.

**Photodimer D1:** Colorless solid; m.p. 214–216 °C. <sup>1</sup>H NMR (400 MHz, CDCl<sub>3</sub>, 30 °C): δ = 2.00 (m, 4 H, CCH<sub>2</sub>C), 3.50–3.80 (m, 16 H, OCH<sub>2</sub>, NCH<sub>2</sub>), 4.59 (s, 2 H, aromatic 10-H), 5.06 (s, 2 H, aromatic 9-H), 5.74 (t, *J* = 6 Hz, 2 H, NH), 6.81–6.86 (m, 6 H, aromatic 3-, 6-, 7-H), 6.89 (dd, *J* = 7.8, 1.5 Hz, 2 H, aromatic 2-H), 6.94 (dd, *J* = 5.7, 3.0 Hz, 2 H, aromatic 5-H), 6.98 (dd, *J* = 7.4, 1.4 Hz, 2 H, aromatic 4-H), 7.16 (dd, *J* = 5.6, 3.0 Hz, 2 H, aromatic 8-H) ppm. <sup>13</sup>C NMR (100 MHz, CDCl<sub>3</sub>, 30 °C): δ = 30.3, 37.3, 50.2, 53.7, 68.6, 70.4, 70.5, 123.6, 125.7, 125.9, 126.0, 126.6,

127.5, 128.8, 134.4, 142.8, 143.3, 144.7, 169.4 ppm. MS (ESI): *m/z* = 651.48 [M + Na]<sup>+</sup>.

**Photodimer D2:** Pale yellow solid; m.p. 216–218 °C. <sup>1</sup>H NMR (400 MHz, CDCl<sub>3</sub>, 30 °C): δ = 2.00 (m, 4 H, CCH<sub>2</sub>C), 3.54–3.82 (m, 16 H, OCH<sub>2</sub>, NCH<sub>2</sub>), 4.61 (s, 2 H, aromatic 10-H), 5.23 (s, 2 H, aromatic 9-H), 6.78–6.82 (m, 4 H, aromatic 6-, 7-H), 6.85–6.92 (m, 6 H, aromatic 3-, 5-, 8-H), 7.00 (dd, *J* = 7.8, 1.3 Hz, 2 H, aromatic 2-H), 7.07 (dd, *J* = 7.4, 1.3 Hz, 2 H, aromatic 4-H), 7.31 (t, *J* = 5.4 Hz, 2 H, NH) ppm. <sup>13</sup>C NMR (100 MHz, CDCl<sub>3</sub>, 30 °C): δ = 29.8, 37.9, 49.9, 53.8, 69.0, 70.2, 70.7, 125.1, 125.70, 125.79, 125.83, 126.8, 127.6, 129.0, 134.5, 141.0, 143.1, 143.4, 145.4, 169.6 ppm. MS (ESI): *m/z* = 651.48 [M + Na]<sup>+</sup>.

**Photodimer D3:** Pale yellow solid. <sup>1</sup>H NMR (400 MHz, CDCl<sub>3</sub>, 30 °C): δ = 1.94 (m, 4 H, CCH<sub>2</sub>C), 3.43–3.82 (m, 16 H, OCH<sub>2</sub>, NCH<sub>2</sub>), 4.60 (d, *J* = 11.2 Hz, 2 H, aromatic 10-H), 5.79 (d, *J* = 11.2 Hz, 2 H, aromatic 9-H), 6.77 (t, *J* = 5.0 Hz, 2 H, NH), 6.78–7.08 (m, 14 H, aromatic 2- to 8-H) ppm. <sup>13</sup>C NMR (100 MHz, CDCl<sub>3</sub>, 30 °C): δ = 28.6, 40.3, 47.5, 53.1, 70.9, 71.4, 73.0, 124.0, 125.2, 125.7, 125.8, 127.1, 127.7, 127.9, 142.7, 142.9, 143.0, 145.8, 169.3 ppm.

**Photodimer D5:** Pale yellow solid; m.p. 256–258 °C. <sup>1</sup>H NMR (400 MHz, CDCl<sub>3</sub>, 30 °C): δ = 1.94 (m, 4 H, CCH<sub>2</sub>C), 3.48–3.84 (m, 16 H, OCH<sub>2</sub>, NCH<sub>2</sub>), 4.70 (d, *J* = 11.2 Hz, 4 H, aromatic 9-, 10-H), 6.90–7.40 (m, 14 H, NH, aromatic 3- to 8-H), 7.54 (d, *J* = 2.0 Hz, 2 H, aromatic 1-H) ppm. <sup>13</sup>C NMR (100 MHz, CDCl<sub>3</sub>, 30 °C): δ = 28.58, 39.19, 53.43, 53.51, 70.03, 70.29, 71.28, 124.05, 125.89, 126.16, 127.03, 127.23, 134.77, 142.63, 143.88, 147.06, 173.41 ppm. MS (ESI): *m/z* = 651.27 [M + Na]<sup>+</sup>.

**Photodimer D6:** Pale yellow solid; m.p. 256–257 °C. <sup>1</sup>H NMR (400 MHz, CDCl<sub>3</sub>, 30 °C): δ = 1.93 (m, 4 H, CCH<sub>2</sub>C), 3.51–3.97 (m, 16 H, OCH<sub>2</sub>, NCH<sub>2</sub>), 4.66 (s, 2 H, aromatic 10-H), 4.67 (s, 2 H, aromatic 9-H), 6.90–6.95 (m, 4 H, aromatic 6-, 7-H), 6.99–7.03 (m, 6 H, aromatic 3-, 5-, 8-H), 7.04 (s, 2 H, aromatic 1-H), 7.16 (t, *J* = 5.2 Hz, 2 H, NH), 7.36 (m, 2 H, aromatic 4-H) ppm. <sup>13</sup>C NMR (100 MHz, CDCl<sub>3</sub>, 30 °C): δ = 28.26, 38.66, 53.49, 53.64, 69.94, 69.97, 70.60, 124.95, 125.13, 125.21, 125.91, 127.25, 132.69, 142.46, 142.67, 143.73, 146.55, 167.16 ppm. MS (ESI): *m/z* = 651.27 [M + Na]<sup>+</sup>.

**<sup>1</sup>H and <sup>13</sup>C NMR Measurements:** <sup>1</sup>H and <sup>13</sup>C NMR spectra were recorded with a JEOL JMM-EX400 spectrometer at 30 °C. The concentrations of the reagents were 1 × 10<sup>−3</sup> mol·dm<sup>−3</sup> in [D<sub>1</sub>]chloroform or [D<sub>3</sub>]acetonitrile. To record spectra of the metal complexes, excess amounts of the metal cations were added as perchlorate salts to these solutions.

**Measurement of Fluorescence and UV/Vis Spectra:** Fluorescence spectra were recorded with a Shimadzu RF-5300PC instrument at 25 °C. The concentrations of the reagents were 1 × 10<sup>−5</sup> mol·dm<sup>−3</sup> in acetonitrile (spectral grade) for **1** and in acetonitrile/DMF (90:10, v/v) (spectral grade) for **2**. Alkali and alkaline earth metal ions were added to the solution of the reagent as perchlorate salts. The temperature was maintained at 25 °C. UV/Vis spectra were recorded with a Shimadzu UV-2400 spectrophotometer with a temperature maintained at 25 °C.

## Acknowledgments

We thank the Center for Instrumental Analysis, Hokkaido University, for instrumentation assistance (elemental analysis and ESI mass spectra).

- [1] F. D. Greene, S. L. Misrock, J. R. Wolfe, *J. Am. Chem. Soc.* **1955**, *77*, 3852–3855.
- [2] D. E. Applequist, M. A. Lintner, R. Searle, *J. Org. Chem.* **1968**, *33*, 254–259.
- [3] S. L. S. Rita, O. C. Dwaine, W. S. Walter, *J. Phys. Chem.* **1975**, *79*, 2087–2092.
- [4] A. Castellan, R. Lapouyade, H. Bouas-Laurent, J. Y. Lallemant, *Tetrahedron Lett.* **1975**, *29*, 2467–2470.
- [5] H. Sasaki, S. Kobayashi, K. Iwasaki, S. Ohara, T. Osa, *Bull. Chem. Soc. Jpn.* **1992**, *65*, 3103–3107.
- [6] H.-D. Becker, *Chem. Rev.* **1993**, *93*, 145–172.
- [7] H.-D. Becker, V. Langer, *J. Org. Chem.* **1993**, *58*, 4703–4708.
- [8] S. Grimme, S. D. Peyerimhoff, H. Bouas-Laurent, J. P. Desvergne, H.-D. Becker, S. M. Sarge, *Phys. Chem. Chem. Phys.* **1999**, *1*, 2457–2462.
- [9] M. J. Moreno, E. Melo, *J. Phys. Chem. B* **1999**, *103*, 10711–10717.
- [10] T. Ojima, H. Akutsu, J. Yamada, S. Nakatsuji, *Polyhedron* **2001**, *20*, 1335–1338.
- [11] D. Cao, H. Meier, *Angew. Chem. Int. Ed.* **2001**, *40*, 186–188.
- [12] D. S. Tyson, C. A. Bignozzi, F. N. Castellano, *J. Am. Chem. Soc.* **2002**, *124*, 4562–4563.
- [13] S. Nakatsuji, T. Ojima, H. Akutsu, J. Yamada, *J. Org. Chem.* **2002**, *67*, 916–921.
- [14] S. Paul, S. Stein, W. Knoll, K. Müllen, *Acta Polym.* **1996**, *47*, 92–98.
- [15] J. R. Jones, C. L. Liotta, D. M. Collard, D. A. Schiraldi, *Macromolecules* **2000**, *33*, 1640–1645.
- [16] M. Mitsuishi, T. Tanuma, J. Matsui, J. Chen, T. Miyashita, *Langmuir* **2001**, *17*, 7449–7451.
- [17] J. T. Goldbach, T. P. Russell, J. Penelle, *Macromolecules* **2002**, *35*, 4271–4276.
- [18] A. Ueno, F. Moriwaki, A. Azuma, T. Osa, *J. Org. Chem.* **1989**, *54*, 295–299.
- [19] M. Usui, Y. Shindo, T. Nishiwaki, K. Anda, M. Hida, *Chem. Lett.* **1990**, 419–422.
- [20] J.-P. Desvergne, M. Gotta, J.-C. Soullignac, J. Laurent, H. Bouas-Laurent, *Tetrahedron Lett.* **1995**, *36*, 1259–1262.
- [21] S. Tamagaki, K. Fukuda, H. Maeda, N. Mimura, W. Tagaki, *J. Chem. Soc., Perkin Trans. 2* **1995**, *2*, 389–393.
- [22] C. E. Bunker, H. W. Rollins, J. R. Gord, Y.-P. Sun, *J. Org. Chem.* **1997**, *62*, 7324–7329.
- [23] J. H. R. Tucker, H. Bouas-Laurent, P. Marsau, S. W. Riley, J.-P. Desvergne, *Chem. Commun.* **1997**, 1165–1166.
- [24] C.-H. Tung, L.-Z. Wu, Z.-Y. Yuan, N. Su, *J. Am. Chem. Soc.* **1998**, *120*, 11594–11602.
- [25] J.-P. Desvergne, H. Bouas-Laurent, E. Perez-Inestrosa, P. Marsau, M. Cotrait, *Coord. Chem. Rev.* **1999**, *185–186*, 357–371.
- [26] G. McSkimming, J. H. R. Tucker, H. Bouas-Laurent, J.-P. Desvergne, *Angew. Chem. Int. Ed.* **2000**, *39*, 2167–2169.
- [27] H. Bouas-Laurent, A. Castellan, J.-P. Desvergne, R. Lapouyade, *Chem. Soc. Rev.* **2000**, *29*, 43–55.
- [28] G. McSkimming, J. H. R. Tucker, H. Bouas-Laurent, J.-P. Desvergne, S. J. Coles, M. B. Hursthouse, M. E. Light, *Chem. Eur. J.* **2002**, *8*, 3331–3342.
- [29] D. Marquis, J.-P. Desvergne, H. Bouas-Laurent, *J. Org. Chem.* **1995**, *60*, 7984–7996.
- [30] T. Tamaki, T. Kokubu, K. Ichimura, *Tetrahedron* **1987**, *43*, 1485–1494.
- [31] C.-H. Tung, J.-Q. Guan, *J. Org. Chem.* **1998**, *63*, 5857–5861.
- [32] C.-H. Tung, L.-Z. Wu, L.-P. Zhang, B. Chen, *Acc. Chem. Res.* **2003**, *36*, 39–47.
- [33] R. Dabestani, J. Higgin, D. Stephenson, I. N. Ivanov, M. E. Sigman, *J. Phys. Chem. B* **2000**, *104*, 10235–10241.
- [34] G. M. J. Schmidt, *Pure Appl. Chem.* **1971**, *27*, 647–648.
- [35] H.-D. Becker, V. Langer, H.-C. Becker, *J. Org. Chem.* **1993**, *58*, 6394–6396.
- [36] Y. Ito, H. Fujita, *J. Org. Chem.* **1996**, *61*, 5677–5680.
- [37] A. Ueno, F. Moriwaki, Y. Iwama, I. Suzuki, T. Osa, T. Ohta, S. Nozoe, *J. Am. Chem. Soc.* **1991**, *113*, 7034–7036.
- [38] F. C. De Schryver, N. Boens, J. Put, *Adv. Photochem.* **1979**, *11*, 359–465.
- [39] A. Nakamura, Y. Inoue, *J. Am. Chem. Soc.* **2003**, *125*, 966–972.
- [40] R. Tahara, T. Morozumi, H. Nakamura, M. Shimomura, *J. Phys. Chem. B* **1997**, *101*, 7736–7743.
- [41] Y. Suzuki, T. Morozumi, H. Nakamura, M. Shimomura, T. Hayashita, R. A. Bartsch, *J. Phys. Chem. B* **1998**, *102*, 7910–7917.
- [42] T. Morozumi, T. Anada, H. Nakamura, *J. Phys. Chem. B* **2001**, *105*, 2923–2931.
- [43] T. Morozumi, H. Hiraga, H. Nakamura, *Chem. Lett.* **2003**, *32*, 146–147.
- [44] H. Hiraga, T. Morozumi, H. Nakamura, *Tetrahedron Lett.* **2002**, *43*, 9093–9095.
- [45] D. W. Marquardt, *J. Soc. Ind. Appl. Math.* **1963**, *11*, 431–441.

Received March 1, 2004